NASA Technical Memorandum 86761

NASA-TM-86761 19850023134

Viscous Flows in Rotating Pipes With Internal Cavities and Related Vortex Breakdowns

D. Weihs

July 1985

National Aeronautics and
Space Administration

NASA Technical Memorandum 86761

Viscous Flows in Rotating Pipes With Internal Cavities and Related Vortex Breakdowns

D. Weihs, Ames Research Center, Moffett Field, California

July 1985

National Aeronautics and
Space Administration

Ames Research Center
Moffett Field, California 94035

VISCOUS FLOWS IN ROTATING PIPES WITH INTERNAL CAVITIES AND RELATED VORTEX BREAKDOWNS

D. Weihs*

Ames Research Center

SUMMARY

The problem of predicting vortex breakdown, which is characterized by a drastic change in core size and trajectory, is still basically unsolved. In the present paper, viscous flow in a long rotating pipe is analyzed, as a model for the type of breakdown observed in wake vortices. The full Navier-Stokes equations are shown to simplify to a set of unlinked partial differential equations. These equations allow for two separate solutions, for both full pipe flows (the classic rotating Hagen-Poiseuille flow) and cavity flows, in which a central area, with no net mass flux or viscous dissipation, is produced. Conditions permitting switching from one type of flow to the other, with no change in the mass flux or velocities at the pipe surface, are found. It is then argued that these conditions indicate when vortex breakdown will occur.

1. INTRODUCTION

The bathtub vortex, with its hollow center, was one of the first observed and best known flow patterns. Swirling flows of liquids in pipes can also produce configurations with hollow centers under certain conditions of mass flux and tangential velocity (refs. 1,2). The free surfaces thus produced can support standing waves (ref. 2), and the flow field obtained is similar in some respects to that obtained when axisymmetric vortex breakdown occurs in tubes. This similarity has already been noticed (refs. 3,4) and related to the possibility of obtaining an example of conjugate flow states. The existence of conjugate flows forms the basis of Brooke-Benjamin's theory of vortex breakdown (ref. 3).

The studies cited above all deal with inviscid flow. In the present work, viscous flow will be examined to investigate the effects of viscosity on the production of hollow cores, as well as to better describe this form of pipe flow as a model for a free vortex core. Thus, we look at the viscous flow inside a rotating tube whose length is much greater than its diamater. This can be seen as an

*NRC Senior Research Associate. Permanent address: Department of Aeronautical Engineering, Technion, Israel Institute of Technology, Haifa, Israel.

idealization of a vortex core, if the coordinate system in which the tube wall is at rest is considered to be moving at the free-stream velocity.

In section 2, the equations of motion are solved for the flow configuration above. Solutions showing cases of cavity flow arising for high swirl ratios are shown (sec. 3) to be a possible model for the inception of vortex breakdown of the axisymmetric kind in vortices of uniform strength. This approach is similar to the quasi-cylindrical, boundary-layer-type analysis (see ref. 5 for a review), in that conditions causing failure of the cylindrical approximation will indicate actual occurrences, such as separation or breakdown, even though the assumptions on which the analysis is based are thereby invalidated.

2. ANALYSIS

To obtain conditions for a change in the flow configuration, we now look at flows with fixed mass flux Q in a tube of fixed radius a. Considering a viscous incompressible fluid, the equations of motion for steady flow in fixed cylindrical coordinates (r, θ, x; see fig. 1) are, after nondimensionalizing,

$$u\frac{\partial u}{\partial x} + v\frac{\partial u}{\partial r} + \frac{w}{r}\frac{\partial u}{\partial \theta} = -\frac{p_\infty}{\rho \tilde{U}^2}\frac{\partial p}{\partial x} + \frac{\nu}{\tilde{U}a}\left[\frac{\partial^2 u}{\partial x^2} + \frac{1}{r}\frac{\partial u}{\partial r}\left(r\frac{\partial u}{\partial r}\right) + \frac{1}{r^2}\frac{\partial^2 u}{\partial \theta^2}\right] \tag{1a}$$

$$u\frac{\partial v}{\partial x} + v\frac{\partial v}{\partial r} + \frac{w}{r}\frac{\partial v}{\partial \theta} = -\frac{p_\infty}{\rho \tilde{U}^2}\frac{\partial p}{\partial r} + \frac{w^2}{r} + \frac{\nu}{\tilde{U}a}\left[\nabla^2 v - \frac{v}{r^2} - \frac{2}{r^2}\frac{\partial w}{\partial \theta}\right] \tag{1b}$$

$$u\frac{\partial w}{\partial x} + v\frac{\partial w}{\partial r} + \frac{w}{r}\frac{\partial w}{\partial \theta} = -\frac{p_\infty}{\rho \tilde{U}^2}\frac{\partial p}{\partial \theta} - \frac{vw}{r} + \frac{\nu}{\tilde{U}a}\left[\nabla^2 w + \frac{2}{r^2}\frac{\partial v}{\partial \theta} - \frac{w}{r^2}\right] \tag{1c}$$

Here ρ and ν are the density and kinematic viscosity, respectively, and u, v, and w are, respectively, the axial, radial, and tangential components of velocity divided by the average speed $\tilde{U}$ defined below. All lengths are normalized by the radius a. The pressure is divided by a reference gauge pressure p_∞, at the entrance; $\tilde{U}$ is defined by

$$\tilde{U} = \frac{\bar{Q}}{\rho \pi a^2} \tag{2}$$

The tube (which can describe the outer boundary of a vortex core) is rotating around its longitudinal axis at speed W. This can be normalized as

$$W = \frac{\tilde{W}}{\tilde{U}} \tag{3}$$

The boundary conditions for equation (1) are, at $r = 1$ (the tube wall),

$$u = 0 \tag{4a}$$

$$v = 0 \tag{4b}$$

$$w = W \tag{4c}$$

and at $r = b$ (the cavity) where $0 \leq b < 1$,

$$\frac{\partial u}{\partial r} = 0 \tag{5a}$$

$$v = 0 \tag{5b}$$

$$\frac{\partial W}{\partial r} = 0 \tag{5c}$$

This is reminiscent of annular Poiseuille flow with the inner cylinder behaving like a free surface. The area covered by $r < b$ will be treated later.

The classic case of rotating Hagen-Poiseuille flow is obtained for $b = 0$ in equation (5). The boundary conditions do not depend on x, so one can assume

$$u \neq u(x) \tag{6}$$

Also, the boundary conditions exhibit axisymmetry so that

$$\frac{\partial}{\partial \theta} = 0 \tag{7}$$

in equation (1) for these cases. From equations (6), (7), the equation of continuity and boundary conditions (4b) and (5b) we obtain:

$$v = 0 \; ; \quad b \leq r \leq 1 \tag{8}$$

and equations (1) reduce to

$$0 = -\frac{p_\infty}{\rho\tilde{U}^2}\frac{\partial p}{\partial x} + \frac{1}{R}\left[\frac{\partial^2 u}{\partial r^2} + \frac{1}{r}\frac{\partial u}{\partial r}\right] \tag{9a}$$

$$0 = -\frac{p_\infty}{\rho\tilde{U}^2}\frac{\partial p}{\partial r} + \frac{w^2}{r} \tag{9b}$$

$$0 = \frac{\partial^2 w}{\partial r^2} + \frac{1}{r}\frac{\partial w}{\partial r} - \frac{w}{r^2} \tag{9c}$$

where R is the Reynolds number ($R = \tilde{U}a/\nu$).

From equation (6) we deduce that $\partial p/\partial x$ is a constant (which we will designate as P_x). Thus, equation (9a) can be solved independently of equations (9b) and (9c). The full solution for (9a) is

$$u = c_3 \ln r + c_2 r^2 + c_1 r + c_0 \tag{10}$$

Substituting equations (4a) and (5a) into (10) we obtain:

$$u = \frac{R\Lambda(-P_x)}{8}(2b^2 \ln r + 1 - r^2) \tag{11}$$

where

$$\Lambda = \frac{2p_\infty}{\rho\tilde{U}^2} \tag{12}$$

is a pressure coefficient.

One can obtain the nondimensional mass flux by integrating the velocity over the tube. This is now done for three cases.

Case 1. <u>The classic Hagen-Poiseuille case (H-P flow)</u>. This case is obtained when $b = 0$, and yields

$$u = \frac{R\Lambda}{8}(-P_x)(1 - r^2) \tag{13}$$

The nondimensional mass flux is then

$$Q_1 = \int_0^{2\pi} \int_0^1 ur\, dr\, d\theta = \frac{\pi}{16} R\Lambda(-P_x) \tag{14}$$

Case 2. No mass-flux in $r < b$ $(0 < b < 1)$. This is the case either when the boundary at $r = b$ is a solid cylinder moving axially at a speed so that $\partial u/\partial r = 0$ at $r = b$, or when a free surface is produced and maintained by rotation of the outer tube. It is the latter case that is of interest. Here, if the pressure is exactly the vapor pressure of the liquid, the internal hollow core is filled by vapor with much lower density, so that the mass flux in $r < b$ may again be neglected. This can also describe cases of axisymmetric vortex breakdown with elongated closed "bubbles" being produced (ref. 6), for the net mass flux in a closed bubble is zero.

The mass flux is now

$$Q_2 = 2\pi \int_b^1 ur\, dr \tag{15}$$

with u taken from equation (11). Integration yields

$$Q_2 = \frac{\pi}{16} R\Lambda(-P_x)(1 + 3b^4 - 4b^2 - 4b^4 \ln b) \tag{16}$$

The third term is alwayys smaller than unity for $0 < b < 1$, and goes to zero when $b = 1$. Thus, for equal mass flux, the pressure gradient in this case has to be larger than that for the H-P flow in the same tube. If we define the pressure gradient ratio for a given fixed mass flux to be

$$\alpha = \frac{(-P_x)\ \text{H-P}}{(-P_x)\ \text{annulus}} \tag{17}$$

we can obtain the following relation (shown in fig. 2) between this ratio and the cavity radius b:

$$\alpha = 1 + 3b^4 - 4b^2 - 4b^2 \ln b \tag{18}$$

Case 3. Uniform flow in $r < b$ (internal plug flow). This case is a good approximation to the situation in which part of the flow is turbulent (at $r < b$). As such, the equivalent viscosity is much higher (eddy viscosity) in this part of the tube, and the velocity gradients much smaller. We thus approximate the flow in $r < b$ to have a uniform axial velocity, obtained by substituting $r = b$ in equation (11)

$$u_b = \frac{R\Lambda}{8}(-P_x)[2b^2 \ln b + 1 - b^2] \tag{19}$$

The nondimensional mass flux is now obtained by

$$Q_3 = 2\pi \int_o^b u_b r\, dr + 2\pi \int_b^1 ur\, dr \tag{20}$$

where u is taken from equation (11). After integration, we obtain

$$Q_3 = \frac{\pi}{16} R\Lambda(-P_x)[1 - b^2]^2$$

Again, defining the ratio of pressure gradients as β,

$$\beta = \frac{(-P_x)\ \text{H-P}}{(-P_x)\ \text{turbulent core}} = (1 - b^2)^2 \tag{21}$$

The variation of β with b also appears in figure 2.

Returning to equation (9), we now solve equation (9c). This can be recast as

$$r^2 \frac{\partial^2 w}{\partial r^2} + r \frac{\partial w}{\partial r} - w = 0 \tag{22}$$

which is an Euler equation, with solutions

$$w = \frac{c_1}{r} + c_2 r \tag{23}$$

Applying boundary condition (4c), and requiring that the free surface at $r = b$ be stress-free we have

$$r = 1 ; \qquad w = W \tag{24a}$$

$$r = b ; \qquad \frac{\partial w}{\partial r} = 0 \tag{24b}$$

as the boundary conditions that equation (23) has to fulfill. The result is

$$w = W\left(\frac{b^2}{1+b^2}\frac{1}{r} + \frac{r}{1+b^2}\right) \tag{25}$$

which gives, when $b = 0$,

$$w = Wr \tag{26}$$

as expected. Equation (25) can now be substituted into equation (9b) to obtain the radial pressure gradient:

$$\frac{\partial p}{\partial r} = \frac{\Lambda}{2}\frac{w^2}{r} = \frac{\Lambda}{2}\frac{W^2}{(1+b^2)^2}\left(\frac{b^4}{r^3} + 2\frac{b^2}{r} + r\right) \tag{27}$$

The pressure difference in the radial direction is

$$\Delta p = \int_b^1 \frac{\partial p}{\partial r}\,dr = \frac{\Lambda}{4}\frac{W^2}{(1+b^2)^2}\left(1 - 4b^2\,\text{ln}\,b - b^4\right) \tag{28}$$

When $b = 0$ (no cavity) the pressure difference is

$$\Delta p = \frac{\Lambda}{4}W^2 \tag{29}$$

so that for $0 < b < 0.528$ the pressure difference in the radial direction is greater in the case of cavity flow than for the regular rotating pipe flow, and for $0.528 < b < 1$ it is less (see fig. 3). The nondimensional stress on the outer pipe wall in the tangential direction is

$$\tau_w = \frac{1}{R}\left.\frac{\partial w}{\partial r}\right|_{b=1} = \frac{W}{R}\frac{1-b^2}{1+b^2} \tag{30}$$

where τ_w is the shear stress acting on this pipe; therefore, the torque on the tube is less for all cavity sizes than for full pipe flow.

The stability of the flow field described by equations (11) and (25) was checked, by means of the so-called Rayleigh, Synge, and Howard-Gupta criteria (ref. 7). No axisymmetric instability was found, so that cavity flow behaves like Hagen-Poiseuille flow in this respect.

3. COMPARISON WITH EXISTING WORK

In the previous section, solutions were developed for viscous pipe flow with swirl allowing for an internal axisymmetric free surface. Increasing the axial pressure gradient for given tube mass flux and tangential velocity can cause the flow to develop an internal axisymmetric cavity, or cause an existing cavity to grow radially. This is in qualitative agreement with experimental results by Escudier et al. (ref. 1) who caused growth of the bubble diameter by putting a sudden contraction in the pipe diameter (which causes an axial acceleration corresponding to an increase in the pressure gradient). Quantitative agreement is not to be expected here, for the experimental setup was somewhat different. In the experiment, there was rotating flow in a stationary pipe, and the tube in the theoretical model represents the edge of the vortex core in the experiment. Nevertheless, as we shall see, various experimental observations can be reproduced in an encouraging manner.

The radial pressure difference across the pipe is given by equation (27) and is shown in figure 3. As we can see, in the range $0 < b < 0.528$ there are, for a given fixed mass flux, always two cavity diameters that result in the same radial pressure difference. As a specific example, take the case $b = 0$. This describes rotating Hagen-Poiseuille flow. A change in the axial pressure gradient, by a factor of 3.16 (fig. 2) results in a flow with a nondimensional cavity radius of $b = 0.528$, having the same radial pressure difference between the center of rotation and the tube wall. This means that removing the outside tube wall would not result in any change in the radial direction (so that this could model a viscous vortex core in a fluid instead of in a solid tube).

The axial pressure drop along the pipe is the viscous analog to Brooke-Benjamin's "flow-force" (ref. 3). This is more aptly seen here as a kind of "availability" in the thermodynamic sense because of the dissipation resulting from viscosity--as manifested by the longitudinal pressure gradient. Thus, the cavity ($b = 0.528$) flow has to lose more energy to traverse a given length. Having less available energy, the cavity flow can be seen as the subcritical conjugate in Brooke-Benjamin's terminology. Although the results above are mathematically rigorous, at the present time our view is that the analogy should be treated as an explanatory device only.

4. ORIGIN OF CAVITY FLOW AND ITS RELATION TO VORTEX BREAKDOWN

As mentioned in the Introduction, the pipe flow of case 2 (sec. 2) can serve as a model for flow in the vortex core, if the outside wall is considered to move at the speed of the potential flow external to the core. The internal mass flux is then the axial flow obtained in the vortex core (ref. 8).

For flow in the tube, the pressure at the outside wall diminishes in the downstream direction along the tube axis (see fig. 4). It follows that at some point x_c the pressure at the wall will be exactly equal to

$$p_c = \frac{\Lambda}{4} W^2 \tag{31}$$

When this point is reached, the pressure at the tube center vanishes (see eq. (29)); that is, a cavity can potentially be formed. Equation (31) can be used to establish a position at which the cavity solution is first obtained, if the pressure at the outlet is taken as zero. This position is a function of the inlet pressure (the reference pressure p_∞ used in the definition of Λ), the mass flux, and the tangential velocity ratio. Written in terms of the present nondimensional quantities, this is

$$(-P_x)X_c = p_\infty - p_c \tag{32}$$

The ambient pressure at the pipe outlet was taken to be zero so one can write $p_\infty = (-P_x)L_o$, where L_o is the length of a fictitious tube along which the total pressure excess is lost to friction. The length L_o is greater than any real tube that sustains a given mass flux. Substituting this relation, as well as equation (31), into (32) we obtain

$$p_c = (-P_x)(L_o - x_c) \tag{33}$$

For full pipe flow (rotating Hagen-Poiseuille flow) the pressure gradient $(-P_x)$ can be obtained from equation (14). As a result, equation (33) can be written as

$$L_o - x_c = \frac{\pi}{64} \frac{R\Lambda^2 W^2}{Q_1} \tag{34}$$

Length L_o has to be, as mentioned above, greater than the real tube length. Putting the actual tube length as x_c in equation (34) will thus define minimum values of the parameters for a cavity to exist. The point at which a cavity can first be sustained is thus a function of the swirl ratio W, the Reynolds number, and the mass flux.

The next step is to attempt to relate the findings above to vortex breakdown, which is essentially a two- or three-dimensional phenomenon, whereas up to now the analysis was one-dimensional. As a result, we cannot expect predictions of the actual postbreakdown flow, but we suggest that the axial position of the breakdown is related to the critical point obtained above. Once zero pressure is obtained, any further drop in pressure is impossible. The constant axial pressure gradient required to fulfill equation (6) no longer exists, and the one-dimensional flow field has to disappear beyond this point. One can then use the boundary-layer separation analogy as proposed by Hall (ref. 5). It states: "If, at some location

in a quasi-cylindrical vortex core the results show appreciable instead of small axial gradients, there must also be appreciable axial gradients at that location in the corresponding real vortex core, even though the quasi-cylindrical approximation must fail there." On this view, x_c in equations (33) and (34) may be seen as an approximation to the breakdown position, with an accuracy of $O(1/x_c)$. Our results can therefore only be qualitatively compared with those of Escudier and Zehnder (ref. 9). They forced breakdown at the entrance to the contraction in their apparatus, which is equivalent to the entry zone in the present model, that is, $x_c = 0$. Escudier and Zehnder showed that for a fixed breakdown position, the Reynolds number, mass flux, and circulation can be related by means of an expression of the form (in present notation)

$$RW^{\gamma}Q^{\delta} = \text{const} \tag{35}$$

where γ and δ are empirically obtained values. As mentioned above, no quantitative comparison is possible (also a result of Escudier and Zehnder's technique for producing swirl), but equations (33) and (34) nonetheless show that relationships such as equation (36) can also be obtained for pipe flow.

5. CONCLUDING REMARKS

Where it exists, the free cavity has been shown both experimentally and by an inviscid analysis to be capable of sustaining standing waves (ref. 2). This fact, in addition to the higher dissipation (resulting in lower available energy), indicates that the cavity flow obtained for a constant mass flux may be a viscous subcritical flow in the sense of Brooke-Benjamin (ref. 3). Criticality conditions such as Squire's (see ref. 5) can be retrieved by assuming inviscid flow, but they are not really relevant here.

We thus conclude that equation (35) can be used as an approximate predictive tool for breakdown in columnar vortices. Increasing vortex strength or swirl ratio causes x_c to diminish, resulting in earlier breakdown. This situation can be qualitatively related, in the following sense, to that of vortices in the wake of slender wings or bodies. Increasing the angle of attack for a given configuration causes both vortex strength and swirl ratio to go up, with a corresponding forward movement of the point of breakdown. Increasing sweep angle at a fixed angle of attack causes W to decrease and R and L_o to increase. The point of breakdown is predicted to move rearward, and this is actually observed (ref. 10).

REFERENCES

1. Escudier, M. P.; Bornstein, J.; and Zehnder, N.: Observations and LDA Measurements of Confined Turbulent Vortex Flow. J. Fluid Mech., vol. 98, 1980, pp. 49-63.

2. Keller, J. J.; and Escudier, M. P.: Theory and Observations of Waves on Hollow-Core Vortices. J. Fluid Mech., vol. 99, 1980, pp. 495-512.

3. Brooke-Benjamin, T.: Theory of the Vortex Breakdown Phenomenon. J. Fluid Mech., vol. 14, 1962, pp. 593-629.

4. Escudier, M. P.; and Keller, J. J.: Vortex Breakdown: A Two Stage Transition. Paper No. 23, AGARD Conference Proc. No. 342, 1983, pp. 1-22.

5. Hall, M. G.: Vortex Breakdown. Annu. Rev. Fluid Mech., vol. 4, 1972, pp. 195-218.

6. Sarpkaya, T.: A Review of Recent Studies on Instability and Wave Breaking in Swirling Flows. J. Fluid Mech., vol. 45, 1971, pp. 545-559.

7. Leibowich, S.: A Review of Recent Studies on Instability and Wave Breaking in Swirling Flows. ASME Paper 83-FE-37, 1983.

8. Batchelor, G. K.: Axial Flow in Trailing Line Vortices. J. Fluid Mech., vol. 20, 1964, pp. 645-658.

9. Escudier, M. P.; and Zehnder, N.: Vortex Flow Regimes. J. Fluid Mech., vol. 115, 1982, pp. 105-121.

10. Lambourne, N. C.; and Bryer, D. W.: The Bursting of Leading Edge Vortices - Some Observations and Discussion of the Phenomenon. Aeronautical Research Council (Great Britain), Reports and Memoranda 3282, 1961.

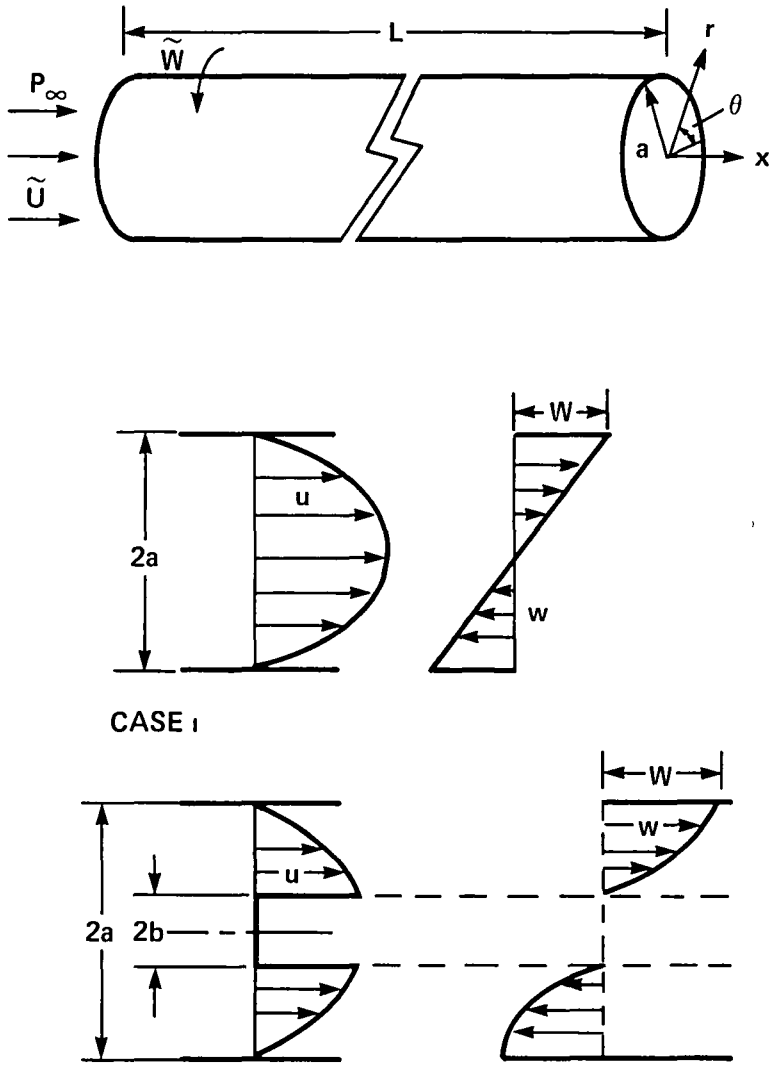

Figure 1.- Schematic representation of pipe flows and cavities.

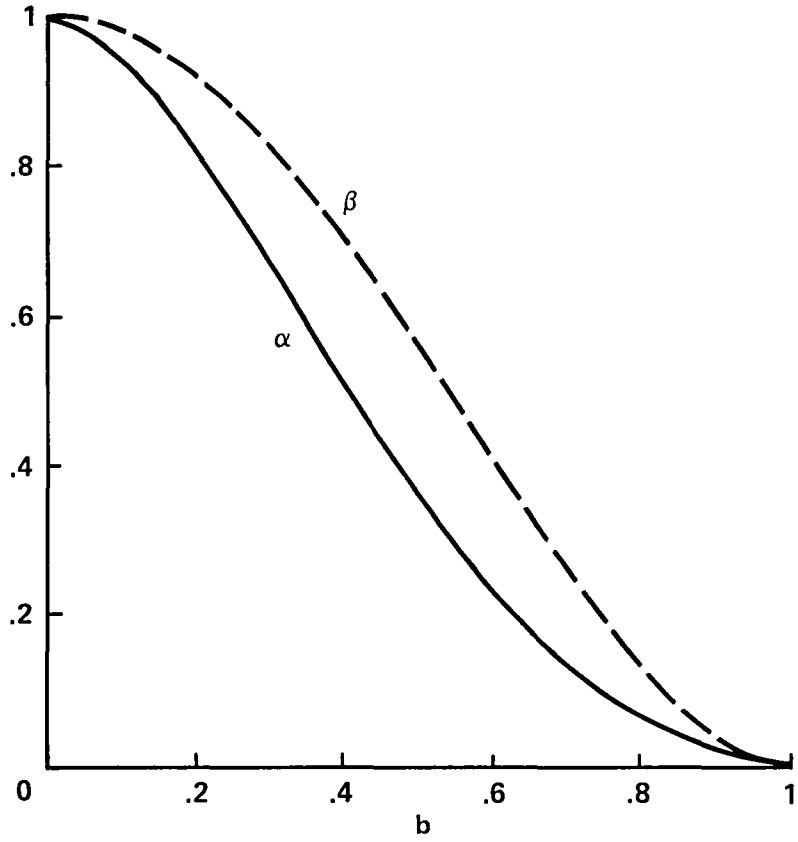

Figure 2.- Ratio of pressure gradients required to drive full, to annular rotating viscous pipe flow α and full laminar, to part turbulent flows β vs. ratio of annulus diameter to pipe diameter b.

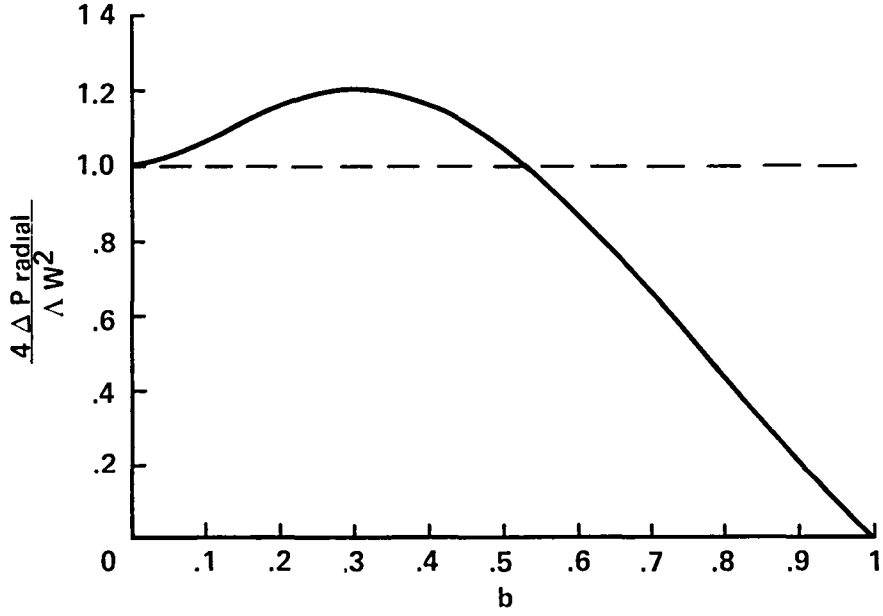

Figure 3.- Pressure increment in the radial direction, normalized by the pressure increment for full rotating pipe flow vs. ratio of annulus diameter to pipe diameter b.

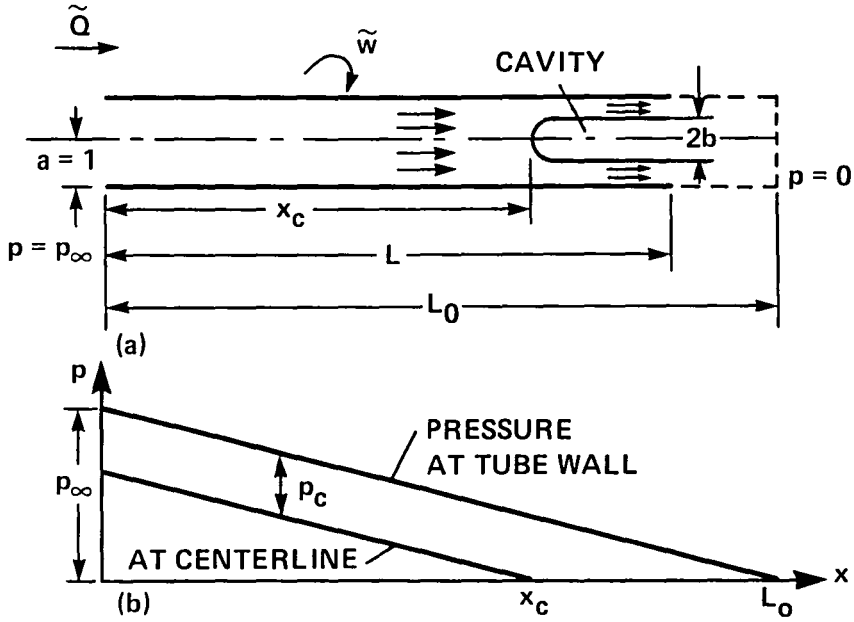

Figure 4.- Schematic representation of pressure distribution and cavity location. (a) Distance to first cavity position x_c, tube length L, and hypothetical maximum tube length L_o (eq. (33)) along which the total pressure excess is lost to friction. (b) Schematic pressure distribution. All lengths are normalized by a, the tube radius.

1 Report No	2 Government Accession No	3 Recipient's Catalog No
NASA TM-86761		

4 Title and Subtitle	5 Report Date
VISCOUS FLOWS IN ROTATING PIPES WITH INTERNAL CAVITIES AND RELATED VORTEX BREAKDOWNS	July 1985
	6 Performing Organization Code
7 Author(s)	8 Performing Organization Report No
D. Weihs, NRC Senior Research Associate*	85282
	10 Work Unit No
9 Performing Organization Name and Address	
Ames Research Center Moffett Field, CA 94035	11 Contract or Grant No
	13 Type of Report and Period Covered
12 Sponsoring Agency Name and Address	Technical Memorandum
National Aeronautics and Space Administration Washington, DC 20546	14 Sponsoring Agency Code 505-31-21

15 Supplementary Notes *Permanent address: Technion, Israel Institute of Technology, Haifa, Israel.
Point of Contact: L. B. Schiff, Ames Research Center, MS 227-6, Moffett Field, CA 94035 (415) 694-6208 or FTS 464-6208

16 Abstract

The problem of predicting vortex breakdown, which is characterized by a drastic change in core size and trajectory, is still basically unsolved. In the present paper, viscous flow in a long rotating pipe is analyzed, as a model for the type of breakdown observed in wake vortices. The full Navier-Stokes equations are shown to simplify to a set of unlinked partial differential equations. These equations allow for two separate solutions, for both full pipe flows (the classic rotating Hagen-Poiseuille flow) and cavity flows, in which a central area, with no net mass flux or viscous dissipation, is produced. Conditions permitting switching from one type of flow to the other, with no change in the mass flux or velocities at the pipe surface, are found. It is then argued that these conditions indicate when vortex breakdown will occur.

17 Key Words (Suggested by Author(s))	18 Distribution Statement
Viscous flow Vortex breakdown Pipe flows Vortex flows	Unlimited Subject Category - 34

19 Security Classif (of this report)	20 Security Classif (of this page)	21 No of Pages	22 Price*
Unclassified	Unclassified	17	A02

*For sale by the National Technical Information Service, Springfield, Virginia 22161

End of Document